MODELING OF THE TEMPORAL BEHAVIOR OF THE SURFACE TEMPERATURE OF AN ISOLATION MATERIAL TEST SAMPLE UNDER AN AC LOW CURRENT ARC

Daniel Fiß[1]; **Stefan Kühnel**[2]; **Ernest Krzyszkowski**[3]; **Stefan Kornhuber**[4]
Hochschule Zittau/Görlitz, University of Applied Science,

[1, 3] Institute of Process Technology, Process Automation and Measurement Technology (IPM)
Department Measuring Technology / Process Automation

[2, 4] Faculty of Electrical Engineering and Informatics
Department for High-Voltage Engineering / Materials / Electromagnetic Theory

Theodor-Körner-Allee 16, 0273, Zittau, Germany
e-mail: [1]d.fiss@hszg.de; [2]s.kuehnel@hszg.de; [3]ernestkk1996@gmail.com;
[4]s.kornhuber@hszg.de

Abstract

In this article, a computational model is presented which can be used to predict the heating of insulating material surfaces by low-current high-voltage arcs. The discharge is represented by a so-called three-cylinder model. Based on this, the heat flows onto the insulating material surface and its heating by means of thermal conduction and convection are calculated. The calculation results are compared to the measurements of the surface temperature on a model arrangement. The overall model reproduces the dynamic behavior of the heating very well. The quantitative deviations from the measurement are only in the range of a few percent.

Keywords

Low current high voltage arcing; Modeling; Heating of insulating material surfaces; Electrical polymer insulating materials; Arc resistance.

Introduction

The use of polymeric insulating materials as housing materials for components in medium and high voltage applications is widespread. These offer various advantages compared to glass or porcelain components [1]. When polymeric insulating materials are used for outdoor applications, they are exposed to various environmental influences that can lead to degradation of the insulating material. Accordingly, these materials must meet various minimum requirements with regard to their properties (e.g., UV resistance) [2]. Especially in outdoor applications and under severe indoor conditions, contamination layers may be deposited on the surface, which contains electrically conductive particles (e.g., salts). If the material does not exhibit hydrophobic properties or has temporarily lost them, a conductive pollution layer can be formed by the presence of moisture. As a result, electrical surface discharges, so-called dry band discharges or high voltage arcs, can occur. The insulating materials used under these conditions must have sufficient resistance to such discharges. This is verified for AC applications by means of various test methods (e.g., inclined plane test according to IEC 60587 [3], high-voltage arc test according to IEC 61621 [4]).

Tests of the tracking and erosion resistance with DC voltage usually show both considerably greater damage and a greater scatter of results [5]. It is assumed this is caused by be a higher local and temporal stability of the discharges as well as a higher power transfer [6], [7]. The

thermal effect of low-current surface discharges is considered to be the main effect of damage or decomposition of polymer insulating materials. [8], [9], [10].

Based on this assumption, a thermal model is developed to calculate the heating of insulating material surfaces by electrical surface discharges. This model should allow conclusions on the thermal stress of insulating material surfaces and support the interpretation of measurement results, especially on the influence of the voltage type. Furthermore, the evaluation of different influencing factors on the heating (thermal conductivity of the insulating material) should be made possible and e.g., a specific material optimization for DC voltage applications should be facilitated. The knowledge gained on the basis of the model also flows into the development of a test procedure for evaluating the DC erosion and tracking resistance.

In the first step, a model is used for an AC arc and a geometrically simplified electrode arrangement with an inert insulating material. In the future, the model will be extended to include more complex geometries, insulation decomposition, DC stress, and sensitivity studies will be performed.

1 Model Test Setup and Temperature Measurements

As a simple geometric experimental arrangement, the electrode arrangement of the high voltage arc test according IEC 61621 [4] is used, as shown in Fig. 1. A low-voltage arc (3) is ignited between two tungsten electrodes (1). The heat of the hot plasma is transferred to the surface of the ceramic test specimen (2) by heat radiation, convection and conduction. Convection is the dominant effect [11]. For the heat distribution in the test specimen, heat conduction is the predominant effect mechanism.

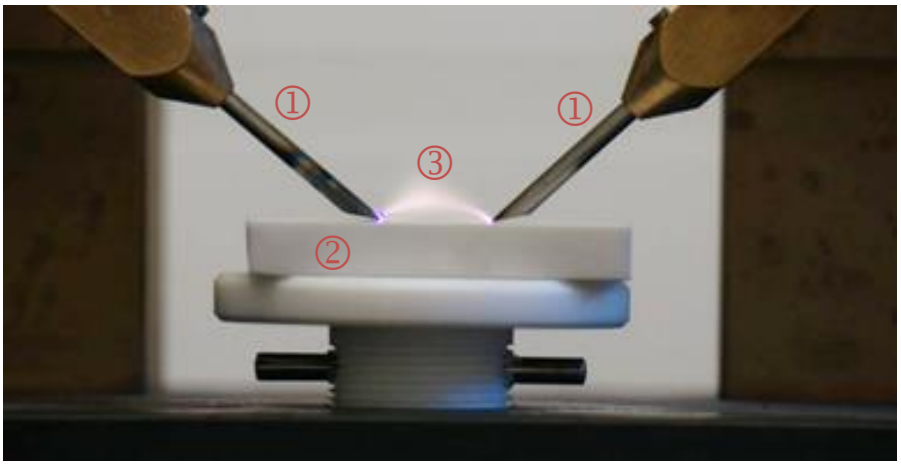

Source: Own

Fig. 1: *Electrode arrangement according IEC 61621: (1) tungsten electrode; (2) ceramic specimen; (3) high voltage arc*

The test voltage of 12.5 kV (rms value) is generated by a high voltage transformer (max. 17 kV, 4.4 kVA). The test circuit is conforming with IEC 61621. The arc current is adjusted by a variable series resistor on the primary side of the transformer. The current is measured by a shunt resistor and recorded by A/D converter. The arc voltage is measured by an ohmic voltage divider and recorded as well. To avoid influences of the arc by the thermal decomposition of the test specimen, an inert test specimen made of aluminum oxide ceramic (Al2O3) with the dimensions 38 mm x 33 mm x 6 mm is used for these experiments. The heating of the test specimen is recorded with a thermal imaging camera “VarioCAM hr head” from InfraTec GmbH and recorded with a measuring frequency of 1 Hz (Fig. 2). The camera is placed at an angle of 90° above the test specimen. The arc is applied to the specimen for 60 minutes overall with continuous temperature measurement.

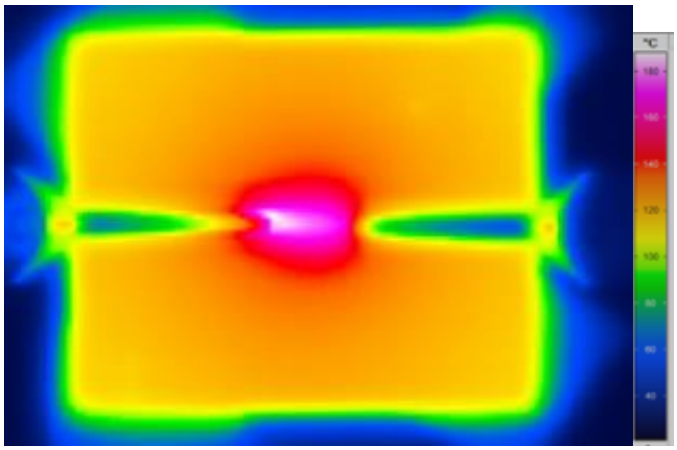

Source: Own

Fig. 2: *Example of a thermogram (20 mA, 500 s)*

At the given geometrical set-up one pixel of the IR camera corresponds to a square of about 0.4 mm of the specimen. The pixels are combined in such a way that they correspond to the size of the nodes of the calculation model. Parameters of the temperature measurement are summarized in Tab. 1.

Tab. 1: *Parameters of the temperature measurement*

Distance to IR camera	48 cm
Angle to surface	90°
Instantaneous Field of View (IFOV)	0.8 mrad
measurement spot size	0.38 mm
Measurement frequency	1 Hz
Emissivity Al_2O_3	0.9

Source: Own

2 Modeling of the Dynamic Behavior of the Surface Temperature for the Experimental Setup

The thermal model of the above-mentioned experimental setup consists of three sub-models that mathematically describe different physical mechanisms. Sub-model 1 describes the arc as a current-voltage model (VCM), the 3-cylinder model (3CM) determines the heat fluxes from the arc to the specimen surface (sub-model 2), and the third (THM) determines the resulting surface temperature due to heat transport within the specimen and to the environment.

The overall model serves the purpose of investigating the influence of the various parameters and their uncertainties on the result.

The sub-models are described in detail in the following sections.

2.1 Sub-Model 1: Arc as Voltage-Current Model (VCM)

If a 50 Hz alternating voltage is applied to the described electrodes it leads to periodical electrical stress to the air gap. If the voltage exceeds the electrical strength of the air a break-through will occur and an electrical discharge is created. The gas is ionized and forms plasma that can reach extremely high temperatures, depending on the carried current. The conditions used in these experiments result in a discharge called a high voltage arc. Using alternating voltage, this process essentially occurs with every change from positive to negative half-wave. If the voltage exceeds a certain amount, the arc ignites. This voltage is defined as ignition voltage U_{t1}, whereby the moment this occurs is called ignition moment t_1. If the

voltage falls below the minimum required for the arc, the extinction voltage U_{t2}, the arc extinguishes. This moment is defined as extinction moment t_2.

The equations are documented in detail in [10]. The characteristic values were determined from the measurement results of the performed experiments. The voltage and current of the arc are described by equations (1) and (2). The sign function "*sign*" is used to take care of the positive and negative half-wave:

$$u_a(t) = \sqrt{2} \cdot U_a \cdot sin(\omega_u \cdot t) \cdot \frac{1+sign((t-t_1)(t-t_2))}{2} + \left[U_{t1} - \frac{U_{t1}-U_{t1}}{t_2-t_1}\right] \cdot \frac{1-sign((t-t_1)(t-t_2))}{2} \quad (1)$$

$$i_a(t) = \sqrt{2} \cdot I_a \cdot sin\left(\omega_i \cdot \left(t - \left(\frac{\pi}{\omega_u} - t_2\right)\right)\right) \cdot \frac{1-sign((t-t_1)(t-t_2))}{2} \quad (2)$$

In the model, interpolation with a 7th-order polynomial is used to describe the part when the arc is ignited. Tab. 2: summarizes the experimentally determined parameters, exemplarily for a test current of 40 mA.

Tab. 2: *Parameters for arc current-voltage model using the example of test current 40 mA*

Parameter	Value	Description
U_a / kV	13	RMS value of the voltage
I_a / mA	40	RMS value of current
U_{t1} / kV	2.1	Ignition voltage
U_{t2} / kV	1.297	Extinguishing voltage
w_u / rad / ms	0.314	Circular frequency of the voltage
w_i / rad / ms	0.314	angular frequency of the current
t_1 / ms	0.402	Ignition moment
t_2 / ms	9.68	Extinguishing moment

Source: Own, inspired by [10]

2.2 Sub-Model 2: Arc as 3-Cylinder Model (3CM)

The 3-cylinder model determines the heat flows that warm the test specimen. The model represents the arc as a straight cylinder. This is divided into three cylinders (zones 1-3), see Fig. 3. The electrical power within the arc forms the basis for the heat flows to the test specimen The electrical power is allocated in equal parts to the three cylinders (zones) as $P_1(t)$, $P_2(t)$ and $P_3(t)$. The respective k-factors determine the weighting of the individual heat flows within the arc ($P_{13}(t)$, $P_{32}(t)$, $P_{31}(t)$, $P_{23}(t)$) as well as those flowing to the electrodes ($P_k(t)$, $P_a(t)$) and the specimen ($P_{1s}(t)$, $P_{2s}(t)$, $P_{3s}(t)$). The physical meaning of the k-factors is explained in [12] and the values are adapted from [10], cf. Tab. 3.

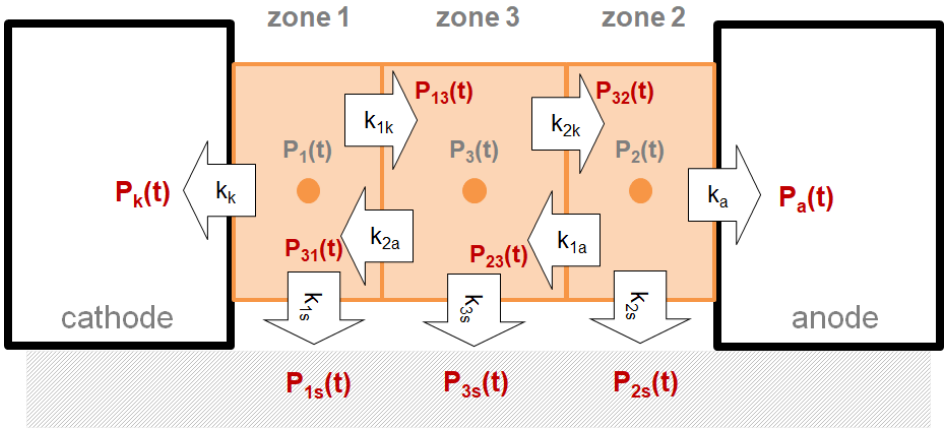

Source: Own, based on [10]

Fig. 3: *Resulting heat flows to the test specimens and the zoning of the 3-cylinder model according to [12]*

The parameters from Fig. 3: have the following meaning:

- $P_k(t)$ – heat flux delivered to the cathode,
- $P_a(t)$ – heat flux delivered to the anode,
- $P_{1s}(t)$, $P_{2s}(t)$, $P_{3s}(t)$ – thermal power transferred from the respective zone to the material surface.
- the corresponding *k*-factors have indices that characterize their source and sink:
  - *a* – the anode,
  - *k* – cathode respectively,
  - *s* – material surface.

As shown in Fig. 3, five heat fluxes result from the arc affecting the specimen and the electrodes. The heat flows from the arc to the rest of the environment are not explicitly calculated. The heat dissipation over the shell surface is primarily weighted by the factors k_{1s}, k_{2s} and k_{3s}. The value of 0.33 defines a heat dissipation of one third of the shell surface to the test specimen. The remaining two thirds of the heat are transferred to the environment. Equations (3), (4) and (5) describe, exemplarily, the calculation of the heat flow $P_k(t)$, which is transferred through the circular surface of the arc cylinder (front surface of the arc at the cathode) via the cathode to the test specimen surface. The parameters are summarized in Tab. 3.

The heat flow to the cathode $P_k(t)$ is composed as follows [10], [12]:

- Heat flow from zone 2 to zone 3:

$$P_{23}(t) = \frac{1}{2} k_{1a} \cdot P_2(t) \cdot \left(1 - \frac{d_2(t)}{\sqrt{a_2(t)^2 + d_2(t)^2}}\right) \tag{3}$$

- Heat flow from zone 3 (incl. zone 2) to zone 1:

$$P_{31}(t) = k_{2a} \cdot \left(P_{23}(t) + \frac{1}{2} P_3(t) \cdot \left(1 - \frac{d_3(t)}{\sqrt{a_3(t)^2 + d_3(t)^2}}\right)\right) \tag{4}$$

- The resulting heat flow from zone 1 (incl. zone 2 + 3) via cathode to test specimen:

$$P_k(t) = \frac{1}{2} k_k \cdot \left(P_{31}(t) + P_1(t) \cdot \left(1 - \frac{d_1(t)}{\sqrt{a_1(t)^2 + d_1(t)^2}}\right)\right) \tag{5}$$

The model was developed for arcs with significantly larger current values [12]. It is being investigated whether the model can also be used for low currents (10 mA - 40 mA) [10].

Tab. 3: *Parameters for the 3-cylinder model*

Parameter	Value	Description
d_1, d_2 [mm]	1	Half cylinder length zone 1 (cathode) and zone 2 (anode)
d_3 [mm]	2.5	Half the cylinder length of zone 3 (arc column)
a_1, a_2, a_3 [mm]	$k_L \cdot i_a(t)$	Radii of the cylinders (product of current $i_a(t)$ and proportionality factor k_L)
k_{1a} [-]	0.2	Weighting coefficient of heat flow from zone 2 to zone 3
k_{2a} [-]	0.2	Weighting coefficient of heat flow from zone 3 to zone 1
k_a [-]	0.3	Weighting coefficient of heat flow from zone 2 to anode
k_{1k} [-]	0.2	Weighting coefficient of heat flow from zone 3 to zone 1
k_{2k} [-]	0.5	Weighting coefficient of heat flow from zone 3 to zone 2
k_k [-]	0.3	Weighting coefficient of heat flow from zone 2 to cathode
k_{1s} [-]	0.33	Weighting coefficient of the heat flux from zone 2 to the test specimen surface
k_{2s} [-]	0.33	Weighting coefficient of the heat flux from zone 2 to the test specimen surface
k_{3s} [-]	0.33	Weighting coefficient of the heat flux from zone 2 to the test specimen surface
k_L [mm / mA]	0.0065	Proportional factor arc diameter to current
L_a [cm]	0.7	arc length

Source: Own, inspired by [10], [12]

Considering the duration of about 1 h until a steady-state surface temperature is established. It makes sense to choose the simulation step size as large as possible. The dynamics of the temperature model is significantly lower than that of the arc as voltage-current model (VCM). The time constants are between 0.01 s and 0.1 s and the period of the sinusoidal oscillation is 20 ms (50 Hz). With a recommended simulation step size of one-tenth of the period duration (Shannon sampling theorem) [13], this results in a constant step size of 0.002 s. This leads to an enormous computational effort (computing time). For this reason, the RMS values of arc current, arc voltage, arc power, and the resulting heat flows are used for further simulations. The investigations show that there are no significant differences in the resulting surface temperature curves compared to the use of the time curves of current, voltage, and power. By using the RMS values, it is possible to perform the simulations with a variable step size depending on the dynamics of the temperature model. This leads to the next chapter of the arc as a temperature-heat model (THM).

2.3 Sub-Model 3: Temperature-Heat Model (THM)

The third sub-model determines the surface temperature of the test specimen from the resulting heat flows. The physical basis is the heat transport within the test specimen and to the environment. Specifically, the mechanisms of convection and heat conduction are considered. Heat radiation from the test specimen to the environment is neglected due to its minor influence [11].

Heat balancing was chosen as the modeling approach. The principle is shown in Fig. 4 and results in differential equation (6). The heat $Q(t)$ for a volume element (node) is considered. The temporal change of this heat depends on the temporally supplied $\dot{Q}_{zu}(t)$ and dissipated heat flows $\dot{Q}_{ab}(t)$.

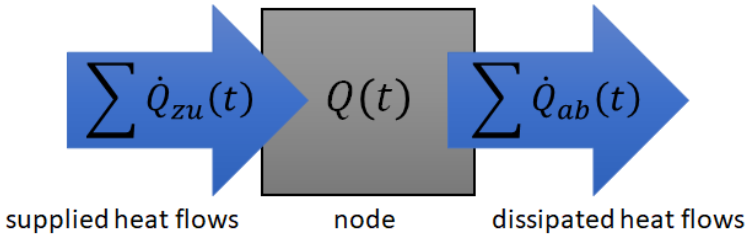

Source: Own

Fig. 4: *Model idea of the heat balancing*

$$\frac{dQ(t)}{dt} = \sum \dot{Q}_{zu}(t) - \sum \dot{Q}_{ab}(t) \tag{6}$$

The specimen is divided into 38 nodes along the arc, as illustrated in Fig. 5. A node has the dimension of 0.001 m x 0.0033 m x 0.0006 m (length x width x height). The remaining test specimen is considered as one large node. For each node, a differential equation is set up, i.e., for 39 nodes, a differential equation system results, which consists of 39 differential equations.

The time-dependent heat $Q(t)$ of a node is described by equation (7).

$$Q(t) = m_{Node} \cdot c_{p_{Node}} \cdot \vartheta_{Node}(t) \tag{7}$$

Equation (7) is the product of the material mass of the node m_{Node}, the heat capacity $c_{\text{p Node}}$ and the temperature of the nodes $\vartheta_{\text{Node}}(t)$. The mass and heat capacity are considered constant.

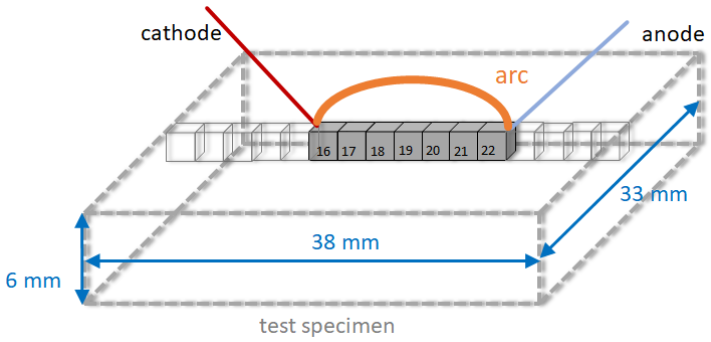

Source: Own

Fig. 5: *Scheme of the node arrangement, arc and test specimen*

In addition to the energy supplied by the arc, the test specimen (between the nodes) is affected by thermal conduction and through the test specimen surface by thermal convection (heat dissipation to the environment). The thermal conductivity $\dot{Q}_{Leit}(t)$ in a homogeneous material is generally defined by equation (8) [14]

$$\dot{Q}_{Leit}(t) = \lambda(t) \cdot A \cdot \left(\frac{d\vartheta_x(t)}{dx}\right)_x \tag{8}$$

where $\lambda(t)$ describes the thermal conductivity of the test specimen material. This is temperature dependent. A is the area to the neighboring node and $d\vartheta_x(t)/dx$ describes the temporal change of the temperature along one dimension (x-axis). By referring to two adjacent nodes, equation (8) becomes equation (9)

$$\dot{Q}_{Leit}(t) = \lambda(t) \cdot A \cdot \left(\frac{\vartheta_{Nb}(t) - \vartheta_{Node}(t)}{\Delta x}\right)_x \tag{9}$$

where $\vartheta_{Nb}(t)$ stands for the temperature of the neighboring node. The distance of the node centers is defined by Δx. The heat convection $\dot{Q}_{konv}(t)$ to the environment is determined by equation (10). The heat transfer coefficient α describes the intensity of heat transfer at the specimen surface and A_O is the surface over which the heat flux flows to the environment [14].

$$\dot{Q}_{konv}(t) = \alpha \cdot A_O \cdot (\vartheta_{Node}(t) - \vartheta_U) \tag{10}$$

With equations (6), (7), (9) and (10) plus a part of the heat flow from the arc, the respective differential equations for the nodes are set up. Three different basic equations crystallize, which differ in the heat fluxes supplied and dissipated. Fig. 6 illustrates the three different types:

- Type A: These are the two nodes on the left and right edges of the specimen. The heat flow supplied is defined by the heat conduction from the neighboring node. Heat is dissipated by convection to the environment and by conduction to the rest of the specimen.
- Type B: Is characterized by the heat supply of the arc. The heat is dissipated to the cooler neighboring nodes by heat conduction. These nodes are located under the arc.
- Type C: These nodes are located between the edge nodes and the under the arc nodes. They absorb heat by conduction from the warmer neighbor and transfer it to the cooler one as well as to the rest of the specimen. Heat is transferred to the environment via the surface by convection.

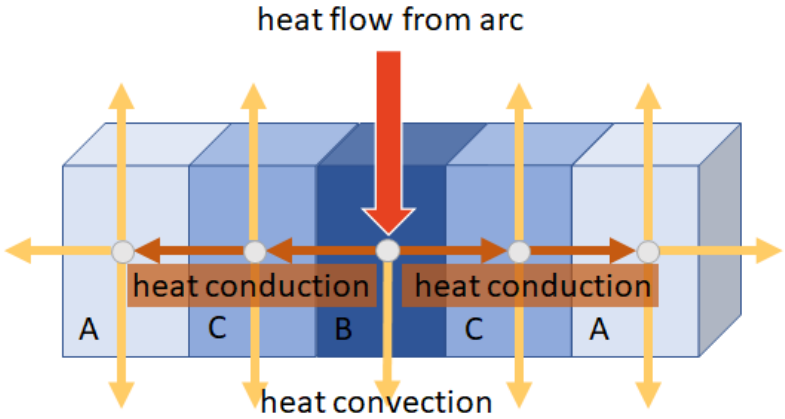

Source: Own

Fig. 6: *Scheme of model representation for the different node types based on the resulting heat balances.*

As an example, the resulting differential equation (11) for type B (nodes under the arc) is given. $\dot{Q}_{LB}(t)$ represents the heat flux from the arc. Equation (11) describes how the temperature of the node $\vartheta_B(t)$ changes in time as a function of the heat fluxes supplied and removed.

$$\frac{m_B \cdot c_{p_B}}{G_B} \cdot \frac{d\vartheta_B(t)}{dt} + \vartheta_B(t) =$$

$$= \frac{1}{G_B} \cdot \dot{Q}_{LB}(t) + \frac{\alpha_B \cdot A_{O_B}}{G_B} \cdot \vartheta_U + \frac{\lambda_{Pr} \cdot A_{lr}}{\Delta x \cdot G_B} \cdot \vartheta_l(t) + \frac{\lambda_{Pr} \cdot A_{lr}}{\Delta x \cdot G_B} \cdot \vartheta_r(t) + \frac{2 \cdot \lambda_{Pr} \cdot A_{Pr}}{h \cdot G_B} \cdot \vartheta_{Pr}(t) \tag{11}$$

where

$$G_B = \frac{\alpha_B \cdot A_{O_B} \cdot \Delta x \cdot h + 2 \cdot \lambda_{Pr} \cdot A_{lr} \cdot h + 2 \cdot \lambda_{Pr} \cdot A_{Pr} \cdot \Delta x}{\Delta x \cdot h} \quad (12)$$

Tab. 4: contains the explanations of the parameters used. The differential equation system is composed of 39 DGL (two type A, seven type B, and 29 type C). For the first studies, it is assumed that the material parameters (thermal conductivity, heat capacity, density, heat transfer coefficient) are independent of temperature.

Tab. 4: *Parameters used in equations (11) and (12)*

Parameter	Explanation
Dx	Distance of the node centers (symmetrical)
h	Node height
A_{lr}	Surface to neighboring node (left and right neighbor)
A_{Pr}	Surface between node and remaining test specimen
A_{OB}	Surface between node and environment
m_B	Mass of a node (density [3800 kg / m³])
l_{Pr}	Thermal conductivity of the test specimen material
c_{pB}	Heat capacity of the test specimen material [950 W / (kg * K)]
a_B	Heat transfer coefficient [12 W / (m * K)]
$\vartheta_B(t)$	Node temperature
$\vartheta_l(t)$	Temperature of the left neighboring node
$\vartheta_r(t)$	Temperature of the right neighbor node
$\vartheta_{Pr}(t)$	average temperature of the remaining test specimen
ϑ_U	Environmental temperature [295 K]

Source: Own

3 Verification and Validation of the Model

The simulations of the temporal behavior are carried out with MATLAB®. The aim is to determine the change in surface temperature over time for different test current levels (10, 20, 30 and 40 mA) and to validate the models using the measured data.

The general model behavior is plausible, with increasing current intensity the surface temperature increases. The surface temperature also reaches a stable steady-state final value. Like mentioned above the model behavior are investigated with the time characteristics of current and voltage and the RMS values. No difference in the resulting surface temperatures was observed.

3.1 Validation of Sub-Model 1: Voltage-Current Model (VCM)

As an example, the validation is carried out with a test current of 40 mA. The curve of the arc voltage is shown in Fig. 7 (left) and of the arc current in Fig. 7 (right). Two periods were shown (40 ms). The blue curves are the experimentally obtained data and the orange curves are the calculated time curves. Fig. 8 shows the curve of the electric arc power. The achieved agreement is qualitatively and quantitatively very good.

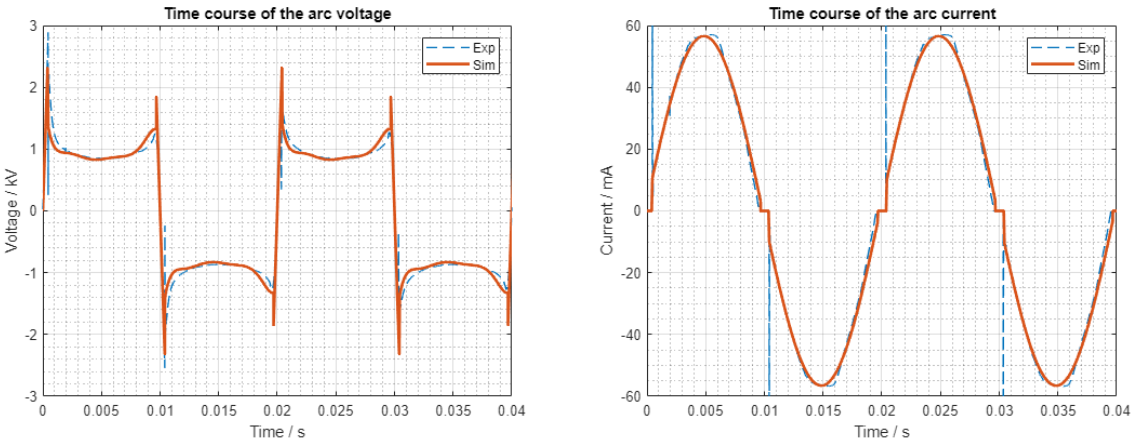

Source: Own

Fig. 7: *Time course of the arc voltage (left) and time course of the leakage current in the arc (right) for a test current of 40 mA: blue – experimental data; orange – simulation data*

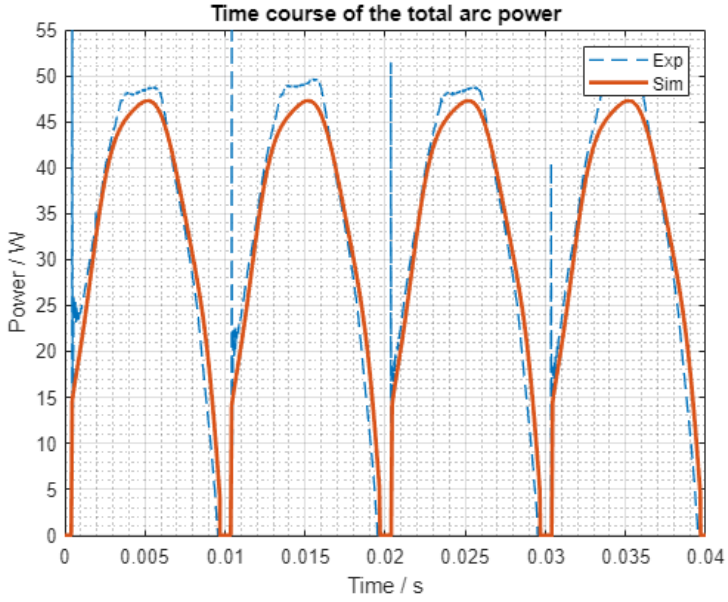

Source: Own

Fig. 8: *Time course of the arc power for a test current of 40 mA: blue – experimental data; orange – simulation data*

When comparing the RMS values of the arc voltage and arc current, cf. Tab. 5, a relative error of approx. 3% is found for the voltage and 1% for the current.

Tab. 5: *Comparison of the rms values of the arc voltage and arc current*

Data source	Arc voltage [kV]	Arc current [mA]	Relative arc voltage [%]	Relative arc current [%]
Experimental data	1.03	40.4	100	100
Model data	0.996	39.97	97	99

Source: Own

3.2 Validation of Sub-Model 2: 3-Cylinder Model (3CM)

To validate the model, heating calculations were first performed with a test current of 10 mA and compared with the measured data. The electrical power of the high-voltage arc is equally distributed for all three cylinder elements (cathode, column and anode), as described in section 2.2. Tab. 6 contains the experimental and calculated data.

Tab. 6: *Data on the distribution of electrical power in the high-voltage arc*

Test current	Data source	Electrical power / W			
		Total	Cathode	Plasma	Anode
10 mA	Experiment	12.1	4.03	4.03	4.03
	Model	12.6	4.20	4.20	4.20
20 mA	Experiment	20.4	6.80	6.80	6.80
	Model	20.9	9.96	6.98	9.96
30 mA	Experiment	29.5	9.83	9.84	9.83
	Model	28.8	9.60	9.60	9.60
40 mA	Experiment	36.2	12.13	12.13	12.13
	Model	35.4	11.80	11.80	11.80

Source: Own

The total power determined from the measured values was used as the output variable. The electrical power at the cathode and anode was calculated from the corresponding voltage drops of the literature. The column voltage was determined from the difference between the total power and the power at the anode and cathode.

3.3 Validation of Sub-Model 3: Temperature-Heat Model (THM)

Fig. 9 illustrates the node distribution under the arc.

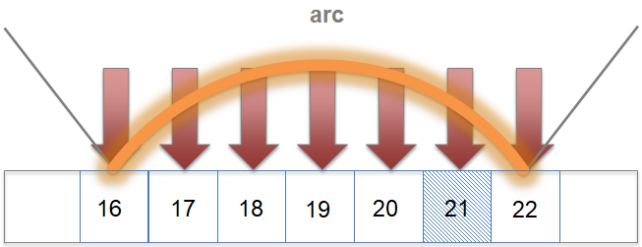

Source: Own

Fig. 9: *Scheme of the node distribution below the arc*

Fig. 10 shows an example of the time curve of the surface temperature in node 21 between the mean value of the experiments and the simulation for an alternating test current of 10 mA. At a time of 30 s, the arc is ignited and there is a very steep rise in the surface temperature. The increase decreases and becomes approximately linear after 40 s. The simulation results mirror the measured values. This shows that the results are within the confidence interval of the averaged values of the tests.

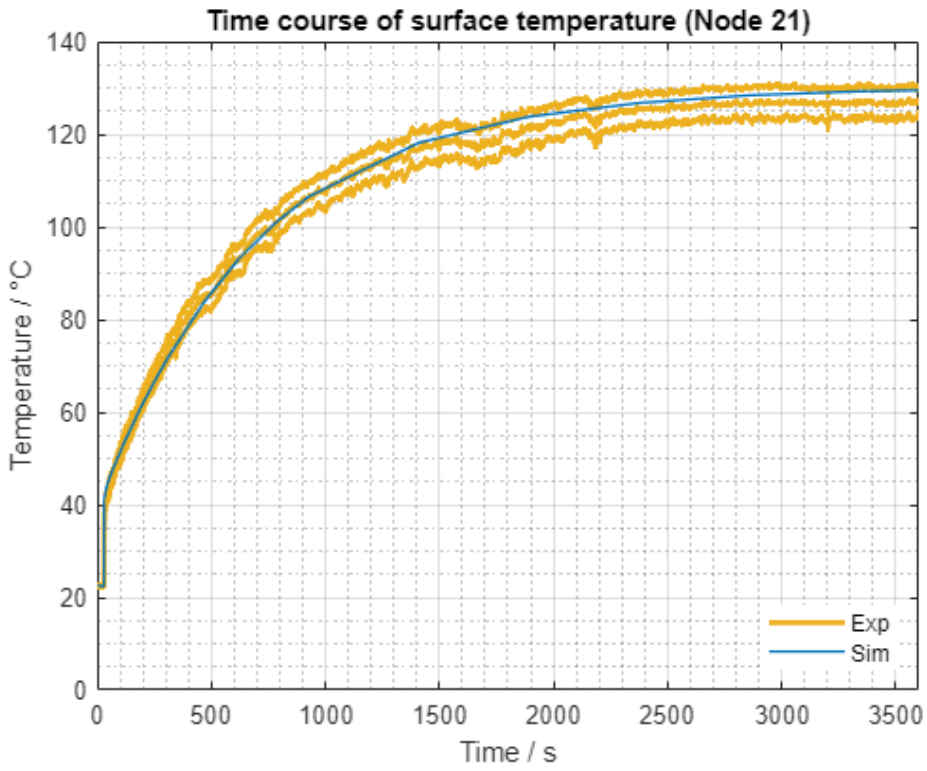

Source: Own

Fig. 10: *Time course of the surface temperature in Node 21 between the mean value of the experiments (with the confidence interval of 95%) and the simulation for a test current of 10 mA*

This becomes clearer in Fig. 11, which shows the deviation over time between the mean value of the experiments and the simulation for all nodes under the arc. The chart shows that the deviations for the nodes at the edge (nodes 16 and 22) are greater than for those in the middle. The largest deviation is about 5 K.

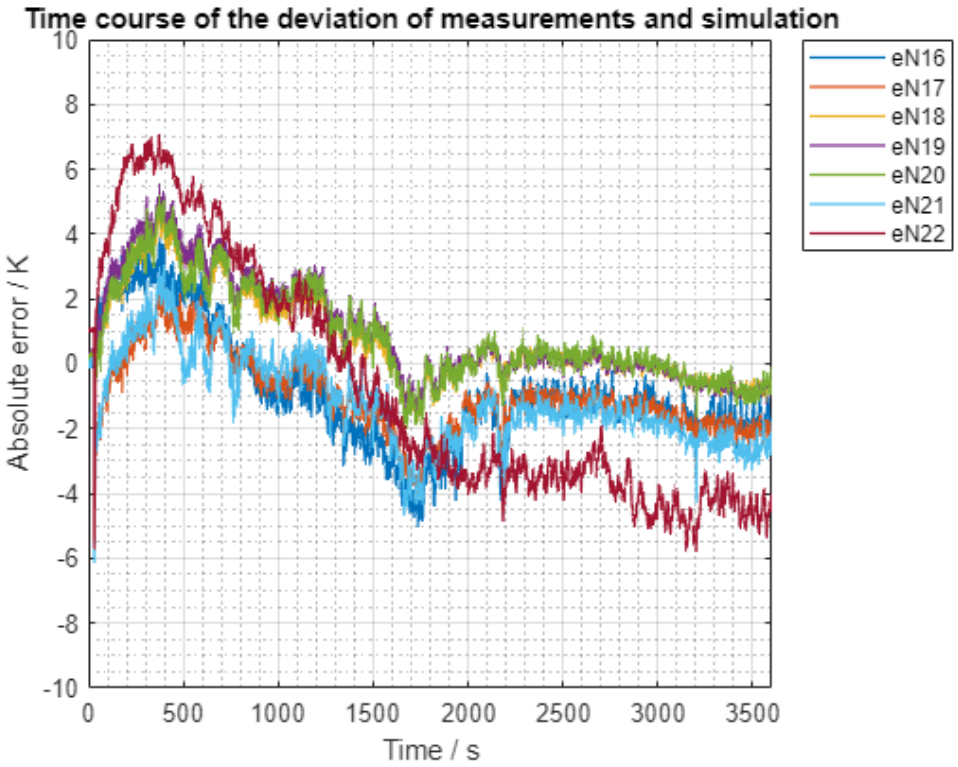

Source: Own

Fig. 11: *Time course of the deviation between the mean value of the experiments and the simulation for all nodes under the arc for a test current of 10 mA*

Analyzing the relative error, shown in Fig. 12, it is clear that the error for the middle nodes (17-21) is in an error band of ±2%. In general, the relative error is smaller than ±5% (green zone). This allows the conclusion that the model reflects the experiments very well and it is suitable for the given experimental constellation to be used as a prediction tool.

In order to minimize the errors, the following improvements are to be investigated in further work. In the next step, the temperature dependence of the material values density, thermal conductivity, heat capacity, and the heat transfer coefficient will be investigated. A further increase of the model accuracy is the increase in the number of nodes.

Finally, the model seems to be suitable to determine the thermal stress caused by electrical surface discharges.

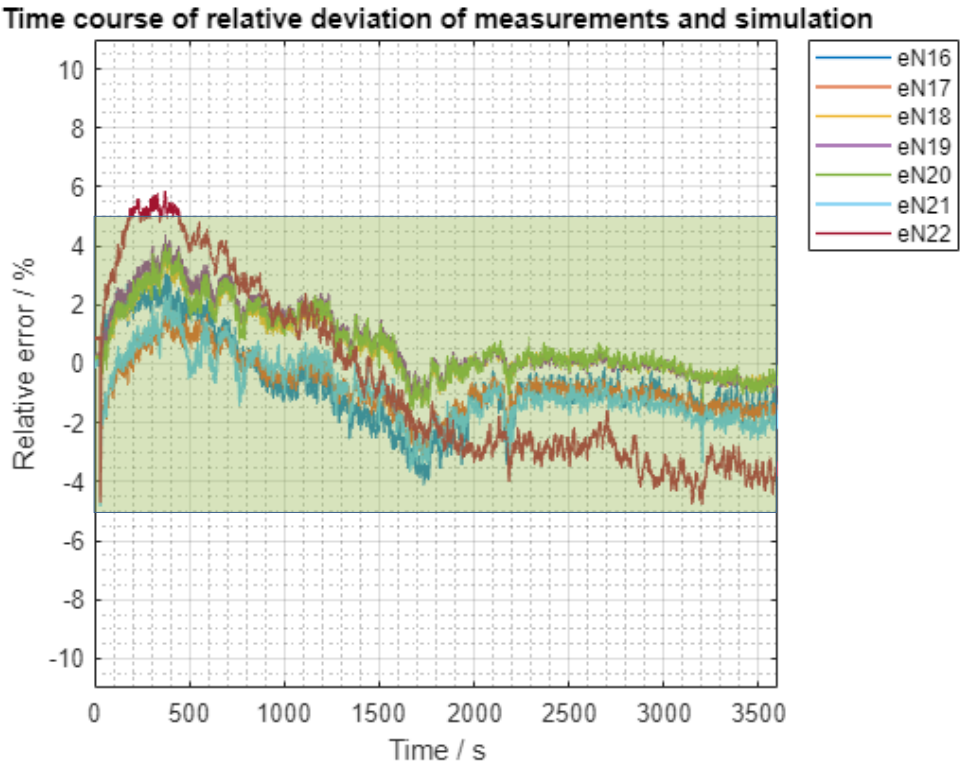

Source: Own

Fig. 12: *Time course of the relative deviation between the mean value of the experiments and the simulation for all nodes under the arc for a test current of 10 mA*

Conclusion

In this article a thermal model is presented which describes the heating of insulation surfaces by low current discharges. The model consists of three parts describing the electrical and thermal characteristic of the arc as well as of heat dissipation to and in the specimen. The model output is compared with experimental data of measurements of the arc voltage and current. Further temperature measurements of with an IR camera are used to verify the model.

The combination of the three sub-models is in very good accordance with the experimental data regarding absolute values and dynamic response. The model was successfully verified and validated. It is concluded that the models are basically applicable to describe the heating of surfaces by low current arcs.

This model will be the base for further investigations and a modification to describe the heating in the case of a DC arc. In a further step, the various influences of the parameters on the surface temperature are explored, and how uncertainties affect the determination of the parameters. A further extension of the model is considered to examine e.g., the effect of material degradation or combustion on the surface heating.

Acknowledgments

The authors would like to acknowledge Hochschule Zittau/Görlitz, University of Applied Sciences for their support of this research.

Literature

[1] PAPAILIOU, K. O.; SCHMUCK F.: *Silikon-Verbundisolatoren – Werkstoffe, Dimensionierung, Anwendungen*. Springer Verlag, Berlin, 2011. ISBN 978-3642238130.

[2] IEC TR 62039 – *Selection guide for polymeric materials for outdoor use under HV stress*. 2007.

[3] IEC 60587:2007 – *Electrical insulating materials used under severe ambient conditions - Test methods for evaluating resistance to tracking and erosion*. 2007.

[4] IEC 61621 – *Dry, solid insulating materials – Resistance test to high-voltage, low-current arc discharges*. 1997.

[5] CIGRÉ WORKING GROUP D1.27: *Feasibility Study for a DC Tracking and Erosion Test*. Technical brochure 611. 2015.

[6] KUEHNEL, S.; KORNHUBER, S.; LAMBRECHT, J.: On the Electrical Characteristic and Heat Dissipation of High Voltage Surface Arcs. *IEEE Conference on Electrical Insulation and Dielectric Phenomena (CEIDP)*. Cancun, Mexico, 2018. DOI: 10.1109/CEIDP.2018.8544746

[7] CERVINKA, R.; BÄRSCH, R.; SEIFERT, J.: Einfluss der Prüfspannungsart auf das Oberflächenverhalten von polymeren Isolierstoffen unter elektrolytischen Fremdschichtbelastungen. *ETG-Fachbericht*. Vol. 125, pp. 69–75. VDE-Verlag Berlin-Offenbach, 2010.

[8] MENZEL, W.: *Zur Klimabeständigkeit von Kunststoff-Innenraumisolierungen mit Oberflächenbeschichtungen*. Dissertation, Technische Hochschule Zittau, 1989.

[9] EL-HAG, A.; MEYER, L. H.; NADERIAN, A.: Experience with Salt-Fog and Inclined-Plane Tests for Aging Polymeric Insulators and Materials. *IEEE Electrical Insulation Magazine*. 2010, Vol. 26, Issue 2, pp. 42–50. DOI: 10.1109/MEI.2010.5482554

[10] ZHANG, X.; ROWLAND, S. M.: Modelling of dry-band discharge events on insulation surfaces. *IEEE International Symposium on Electrical Insulation*. San Diego, CA, USA, 2010. DOI: 10.1109/ELINSL.2010.5549489

[11] KIM, S.-H.; HACKAM, R.: Temperature distribution in RTV silicone rubber coating following band arcing. *Proceedings of 1994 IEEE International Symposium on Electrical Insulation*. Pittsburgh, PA, USA, 1994. DOI: 10.1109/ELINSL.1994.401383

[12] BORKOWSKI, P.; WALCZUK, E.: Thermal Models of Short Arc between High Current Contacts. *Proceedings of the Forth-Seventh IEEE Holm Conference on Electrical Contacts (IEEE Cat. No.01CH37192)*. Montreal, QC, Canada, 2001. DOI: 10.1109/HOLM.2001.953220

[13] KAHLERT, J.: *Simulation technischer Systeme*. Friedr. Vieweg & Sohn Verlag / GWV Fachverlage GmbH, Wiesbaden, 2004. ISBN 978-3-322-80248-4. eBook ISBN 978-3-322-80247-7. DOI: 10.1007/978-3-322-80247-7

[14] VDI e. V.: *VDI-Wärmeatlas*. Springer Vieweg Berlin, Heidelberg, 2013. Series ISSN 2512-5281. Series E-ISSN 2512-529X. DOI: 10.1007/978-3-642-19981-3

MODELOVÁNÍ ČASOVÉHO CHOVÁNÍ POVRCHOVÉ TEPLOTY POVRCHU IZOLAČNÍHO MATERIÁLU PŘI NÍZKOPROUDÉM OBLOUKU

V tomto článku je představen výpočetní model, který lze použít k předpovědi ohřevu povrchů izolačních materiálů nízkoproudými vysokonapěťovými oblouky. Výboj je reprezentován tzv. tříválcovým modelem. Na jeho základě jsou vypočteny tepelné toky na povrchu izolačního materiálu a jeho ohřev pomocí tepelné kondukce a konvekce. Výsledky výpočtu jsou porovnány s měřením povrchové teploty na modelovém uspořádání. Celkový model velmi dobře reprodukuje dynamické chování ohřevu. Kvantitativní odchylky od měření se pohybují pouze v řádu několika procent.

MODELLIERUNG DES ZEITLICHEN VERHALTENS DER OBERFLÄCHENTEMPERATUR EINER ISOLIERSTOFFOBERFLÄCHE UNTER EINEM STROMSCHWACHEN LICHTBOGEN

In vorliegenden Beitrag wird ein Berechnungsmodell vorgestellt, mit welchem die Erwärmung von Isolierstoffoberflächen durch stromschwache Hochspannungs-Lichtbögen vorausberechnet werden kann. Die Entladung wird dabei durch ein sog. Drei-Zylinder-Modell abgebildet. Ausgehend davon werden die Wärmeströme auf die Isolierstoffoberfläche und deren Erwärmung mittels Wärmeleitung und Konvektion berechnet. Die Berechnungsergebnisse werden mit Messungen der Oberflächentemperatur an einer Modellanordnung vergleichend bewertet. Das Modell bildet das dynamische Verhalten der Erwärmung sehr gut ab. Die quantitativen Abweichungen zur Messung liegen lediglich im Bereich weniger Prozente.

MODELOWANIE CZASOWEGO ZACHOWANIA SIĘ TEMPERATURY POWIERZCHNI MATERIAŁU IZOLACYJNEGO POD WPŁYWEM ŁUKU ELEKTRYCZNEGO O NISKIM NATĘŻENIU PRĄDU

W niniejszym opracowaniu przedstawiono model obliczeniowy, który może być stosowany do prognozowania nagrzewania powierzchni materiałów izolacyjnych przez wysokonapięciowe łuki o niskim natężeniu prądu. Wyładowanie jest reprezentowane przez tzw. model trzycylindrowy. Na jego podstawie oblicza się przepływy ciepła na powierzchnię materiału izolacyjnego oraz jego nagrzewanie przy pomocy kondukcji ciepła i konwekcji. Wyniki obliczeń porównane są z pomiarami temperatury powierzchni na układzie modelowym. Cały model bardzo dobrze odtwarza dynamiczne zachowanie ogrzewania. Ilościowe odchylenia od pomiarów są rzędu kilku procent.